

Maunula, T., Ahola, J. and Hamada, H., Reaction mechanism and kinetics of NO_x reduction by propene on CoO_x/alumina catalysts in lean conditions, *Applied Catalysis B: Environmental*, 26 (2000) 173-192.

© 2000 Elsevier Science

Reprinted with permission from Elsevier.

Reaction mechanism and kinetics of NO_x reduction by propene on CoO_x/alumina catalysts in lean conditions

Teuvo Maunula^{a,*}, Juha Ahola^b, Hideaki Hamada^c

^a *Kemira Metalkat, Catalyst Research, P.O. Box 171, FIN-90101, Oulu, Finland*

^b *Department of Process Engineering, University of Oulu, Linnanmaa, FIN-90570, Oulu, Finland*

^c *National Institute of Materials and Chemical Research, 1-1 Higashi, Tsukuba, Ibaraki 305, Japan*

Received 8 September 1999; received in revised form 15 October 1999; accepted 15 January 2000

Abstract

The effect of the preparation method and the Co loading on the performance of alumina supported CoO_x for NO_x reduction by propene was studied in the presence of excess oxygen. Cobalt impregnated on sol–gel γ -alumina (Co/Al-sg) showed higher activity than cobalt on conventional γ -alumina. Co²⁺ was proposed to be the most reactive cobalt phase by catalyst characterization (XRD, XPS). The optimal calcination temperature and Co loading in respect of the NO_x efficiency was found in the specified lean conditions. In general, the calcination temperature of 700°C and the Co loading in the range of 0.8–1.8 wt.% was the optimum by the activity. Static FTIR studies showed the occurrence of several gas phase or surface intermediates like nitrates, oxygenated hydrocarbons and nitrogen–carbon–hydrogen containing species in reaction sequences. The final reactants in the dinitrogen formation have been proposed to be adsorbed NO and an exactly defined nitrogen containing compound denoted as NRO (R=CH₂) in the kinetic model. A derived kinetic model based on reaction experiments and FTIR studies was able to simulate the observed activity results. All the detected gas phase concentrations and proposed surface species coverage were simulated along the Co/Al-sg catalyst bed as a function of temperature with the presented mechanistic kinetic model. © 2000 Elsevier Science B.V. All rights reserved.

Keywords: Nitrogen oxides; Selective reduction; Hydrocarbons; Cobalt; Alumina; Sol–gel; Modeling

1. Introduction

Combustion in lean conditions is a main solution to keep efficiency as high in the utilization of solid or liquid fossil fuels for energy production in mobile or stationary engines or power plants. Catalytic reduction of nitrogen oxides by various methods has been under intense research in the 1990s, because in practice it is very difficult to maintain the high selectivity in NO_x

reduction to nitrogen in the presence of excess oxygen. The interest on Co oxide catalysts was focused at first on their properties to decompose NO, the reaction which has later been studied to understand reaction mechanism [1,2]. Several promising oxide based catalysts have been introduced to reduce nitrogen oxides by hydrocarbons in lean conditions [3–9]. The development degree of catalysts and catalytic processes has now reached the level that no rough technical methods can offer a solution to reach the more demanding emission limits. Low, medium and high temperature NO_x reduction catalysts are needed in different applications

* Corresponding author.

E-mail address: teuvo.maunula@kemira.com (T. Maunula)

and conditions: diesel or lean gasoline fuelled passenger cars (at 150–350°C), trucks (200–600°C) and stationary power plants (250–450°C). Mobile engine applications are very demanding because of the transient driving conditions and the requirement to prevent chemical and hydrothermal deactivation. Cobalt on different supports has been introduced as a promising thermally durable active metal to operate at higher temperatures up to 600°C [10–12]. Alumina [3], silica [10] and zeolites [13] have been examined as supports with cobalt.

The preparation method, Co loading and the type of alumina support are the critical variables for the activity [12,14]. According to the earlier studies, different results for the most active Co phase (CoO, CoAl₂O₄ [10], Co²⁺ [15]) on alumina have been found. The detection of the active forms has varied depending on the precursors, preparation methods, pretreatment conditions and Co loading. The description of the reaction mechanism has been proposed earlier in schematic level [16]. The oxidation of NO to NO₂, the partial oxidation of hydrocarbons and the formation of CN, NCO and nitro intermediates have been proposed to be important steps in NO_x reduction [17]. Various

catalyst and surface characterization methods are the main tools to detect important active sites and reaction intermediates on catalyst surface. The aim in this work was to study the preparation method and reaction mechanism of CoO_x/alumina by activity experiments, characterizations and kinetic modeling.

2. Experimental

2.1. Catalysts

Four different types of alumina (denoted as Al-sg, Al-2, Al-3 and Al-ref) were used as carriers for the catalyst series. The cobalt precursors and concentrations (Al/Co=650–20, molar ratio), as well as the calcination temperature (600–900°C) were varied to find out the influence of these parameters on the catalyst activity and reaction mechanism (Table 1). Al-sg was prepared by sol–gel method and consisted of high surface area γ -Al₂O₃ after calcination at 600°C [18]. Al-2 and Al-3 consist mainly of δ - and α -Al₂O₃, respectively. Co on commercial, conventionally prepared Al-ref (γ -Al₂O₃, Sumitomo) was

Table 1
Composition and surface area of the catalysts^a

Catalyst(Al/Co)	Active metal (wt.%)	Surface area (m ² g ⁻¹)				
		Calcination temperature (°C)				
		600	700	800	900	1000
Co/Al-sg(20)	5.46	196	180	133	117	–
Co/Al-sg(45)	2.50	194	198	146	129	–
Co/Al-sg(65)	1.75	215	180	152	167	116
Co/Al-sg(65, acet)	1.75	223	182	–	–	116
Co/Al-sg(65, wet2)	1.75	204	205	184	–	–
Co/Al-sg 700(65)	1.75	84	–	–	–	–
Co/Al-sg(130)	0.88	199	205	149	132	–
Co/Al-sg(650)	0.18	224	174	–	–	–
Co/Al-2(65)	1.75	84	79	76	75	71
Co/Al-2(65, acet)	1.75	90	82	78	–	78
Co/Al-2/700(65)	1.75	207	–	–	–	–
Co/Al-ref(65)	1.75	150	–	121	–	–
CoO _x	100	–	–	–	–	–
Al-sg (sol–gel γ -alumina)	–	301	243	181	178	178
Al-2 (δ -alumina)	–	99	85	82	81	81
Al-3 (α -alumina)	–	–	–	–	–	–
Al-ref (γ -alumina)	–	162	150	–	–	–

^a Wet2: wet impregnation method 2, other impregnated by wet1; sg: sol–gel; acet: prepared from cobalt acetate, all other impregnated in cobalt nitrate solution.

used as a reference for Co/Al-sg. Cobalt was impregnated by two different type of wet impregnation methods (wet1 and wet2) using $\text{Co}(\text{NO}_3)_2 \cdot 6\text{H}_2\text{O}$ or $\text{Co}(\text{CH}_3\text{COO})_2 \cdot 4\text{H}_2\text{O}$ as precursor salts in aqueous solutions. The amount of solution in wet2 was about the volume needed to fill all pores in Al-sg and in wet1 twice the amount needed for pore filling. Two samples, Co/Al-sg700(600) and Co/Al-2/700(600), were prepared by calcinating alumina (Al-sg and Al-2) at 700°C prior to impregnation and at 600°C after Co impregnation to find the critical point surface modifications during thermal treatments. Commercial, precipitated Co_3O_4 (Soekawa Chemicals) was used as a pure CoO_x material.

2.2. Catalyst characterization and activity measurements

The equipment for activity and a part of characterization (BET, XRD, XRF) experiments were described in our earlier publication [18]. The steady-state activity was evaluated with a gas mixture containing 1000 ppm NO, 1000 ppm propene, 0/10% oxygen and 0/10% water in helium in a temperature range of $200\text{--}550^\circ\text{C}$ (F/W , total flow rate/weight of catalyst = $20\text{ dm}^3\text{ g}^{-1}\text{ h}^{-1}$). 1000 ppm NO_2 or 500 ppm N_2O was also used instead of NO to evaluate the reaction mechanism. The concentrations of N_2 , N_2O , NO, NO_2 , CO_2 , CO, C_3H_6 , C_2H_4 , CH_4 were measured quantitatively by two gas chromatographs and a chemiluminescence NO_x analyzer. The formation of CO_x is also used in figures because both CO and CO_2 were thought to be inert for NO reduction in lean conditions. As soon as hydrocarbon species are reacted to CO or CO_2 , they are no more effective as reductants. Due to the low reactant concentrations, concentration and heat gradients were assumed to be insignificant.

XPS analysis of cobalt containing samples were carried out by using Mg $\text{K}\alpha$ radiation of Rikagaku Denkiogyo XPS-7000 (5 kV, 5 mA, 25 W). The state of Co species was detected by binding energy of Co $2p_{3/2}$ peaks corrected by using a peak of C 1s (285 eV) as a chemical shift reference. The background pressure was 3×10^{-5} mbar at 25°C , which was also the pretreatment condition. Pure Co_3O_4 and $\text{Co}(\text{acac})_2$ (Co^{2+}), as well as CoAl_2O_4 were used as references.

Phase stability of Co/Al-sg(65) and CoO_x samples was examined by a TGA analyzer (Shimadzu

DTG-50) in static air using the following parameters: the sample weight about 20 mg, α -alumina as a reference, the sample holder made from platinum, the heating rate of $10^\circ\text{C min}^{-1}$ in the range of $25\text{--}600$ and $600\text{--}1000^\circ\text{C}$. The sample was kept at a calcination temperature of 600°C for 30 min before the second ramp.

The FTIR adsorption bands on catalyst surfaces were detected at 50, 150, 250 and 350°C by Shimadzu FTIR-8600PC at a resolution of 4 cm^{-1} in the wavenumber range of $4000\text{--}1000\text{ cm}^{-1}$. A thin, compressed sample was installed in a temperature controlled quartz chamber. As a pretreatment the sample was outgassed at 480°C for 30 min and then cooled down to the measurement temperature, at which temperature the background was measured at a pressure below 2.6×10^{-3} mbar. Pure NO (>99%), propene (>99.8%) and oxygen (>99.9%) were introduced into the chamber by two orders: $\text{NO} \rightarrow \text{C}_3\text{H}_6 \rightarrow \text{O}_2$ or $\text{C}_3\text{H}_6 \rightarrow \text{NO} \rightarrow \text{O}_2$. After adsorption at a partial pressure of about 26 mbar for 5 or 10 min, the chamber was evacuated for 5 or 10 min and adsorption bands were measured during both steps. The adsorption measurements of single gases (NO, C_3H_6 , N_2O , CO, CO_2) on these samples at 150 and 350°C and literature data were used as references.

A reaction mechanism based on the observed reactions and surface properties was proposed and rate equations were derived resulting on a kinetic model, which describes all the important concentrations profiles for gas and surface phase reactants. The concentrations of NO (200–1000 ppm), propene (200–3000 ppm) and oxygen (4–10%), space velocity ($20\text{--}240\text{ dm}^3\text{ g}^{-1}\text{ h}^{-1}$) and temperature ($200\text{--}550^\circ\text{C}$) were varied within appropriate ranges in the kinetic activity experiments. The kinetic parameters in the proposed model for tubular reactor were estimated by nonlinear regression analysis.

3. Results and discussion

3.1. Catalytic activity

3.1.1. Significance of precursors and preparation method

Al-sg (γ -form) lost the NO_x activity when increasing the calcination temperature from 600 to 900°C ,

Table 2
The reduction of NO to nitrogen by propene on CoO_x/alumina (Al/Co=65) and alumina catalysts in a dry and wet mixture^a

Sample	Calcination temperature (°C)	Reaction temperature (°C)					
		300	350	400	450	500	550
Co/Al-sg	600	10/7	22/9	53/12	51/28	35/39	14/20
	700	36/–	90/10	88/16	81/49	62/66	23/54
	800	9/7	17/9	70/12	74/28	51/39	17/20
	1000	10/–	25/–	52/–	57/–	46/–	22/–
Co/Al-sg(acet)	600	17/–	21/–	39/–	53/–	45/–	27/–
	700	12/–	18/–	39/–	67/–	50/–	29/–
	800	12/–	15/–	32/–	49/–	48/–	32/–
	1000	6/–	12/–	29/–	43/–	36/–	22/–
Co/Al-sg(wet2)	700	21/–	47/–	87/–	77/–	62/–	29/–
	800	19/–	42/–	84/–	77/–	61/–	40/–
Co/Al-2	600	8/–	12/–	20/–	21/–	18/–	9/–
	700	11/–	18/–	63/–	81/–	65/–	32/–
	800	8/–	11/–	37/–	62/–	56/–	38/–
	1000	6/–	11/–	28/–	49/–	41/–	18/–
Co/Al-2(acet)	600	9/–	14/–	20/–	19/–	18/–	8/–
	700	13/–	20/–	62/–	76/–	60/–	41/–
	800	8/–	11/–	41/–	67/–	53/–	33/–
	1000	7/–	12/–	31/–	53/–	44/–	25/–
Co/Al-ref	600	13/–	19/–	32/–	32/–	20/–	6/–
	800	14/–	21/–	70/–	82/–	69/–	47/–
Al-sg	600	20/9	28/10	35/14	48/20	77/29	33/50
	700	11/–	13/–	21/–	35/–	68/–	54/–
	800	11/–	13/–	22/–	38/–	67/–	39/–
Al-2	600	12/–	15/–	8/–	5/–	6/–	8/–
	700	21/–	26/–	37/–	59/–	90/–	59/–
	800	20/–	27/–	36/–	55/–	92/–	81/–
Al-3	600	2/–	2/–	6/–	6/–	6/–	29/–
	800	–/–	2/–	2/–	2/–	2/–	3/–
Al-ref	600	8/–	8/–	13/–	27/–	60/–	65/–
	700	–/–	10/–	20/–	50/–	86/–	64/–

^a 1000 ppm NO; 1000 ppm C₃H₆; 10% O₂; 0 or 8% H₂O, F/W=20 dm³ g⁻¹ h⁻¹; N₂ formation-%, dry/wet.

because the alumina structure had changed to the direction of less active alumina forms (Table 2). The propene oxidation activity of Al-sg was shifted about 100°C to higher temperatures when calcination temperature increased from 600 to 700°C. The NO reduction activity of Al-2 (δ -Al₂O₃) had a maximum when calcined at 700–800°C. When the catalysts were calcined at 600°C, the NO_x reduction activity of Al-2 based catalysts was low compared to the similar Al-sg based catalysts. The main active sites on both alumina catalysts calcined at over 700°C are expected to be

very similar according to propene oxidation results. Probably the increase from 600 to 700°C alters the hydroxyl groups on the alumina surface [19]. This shift in the oxidation activity had also correlation to NO reactions. As a comparison we studied the performance of α -alumina (Al-3) where the surface area and the amount of surface hydroxyl groups are low. In that experiments with α -alumina the amount of sample was doubled, because the high bulk density of the sample would have caused too large change on the volume and therefore to the flow distribution in the catalyst

bed. Al-3 calcined at 600°C showed same or higher oxidation activity than γ - or δ -forms, but slight NO reduction occurred only at 550°C. No NO reduction activity was detected on α -alumina sample calcined at 800°C. The higher propene oxidation ability can be explained by the higher weight of sample. It can be expected that the loose of active surface sites related to OH groups was a reason for the drop in the propene oxidation activity of γ - and δ -form alumina when they were heated up to 800°C. This deactivation did not happen on α -alumina.

The activities of CoO_x /alumina catalysts for NO reduction by propene in the absence and presence of water were also shown in Table 2. Depending on the metal-support interaction and thermal properties of single phases, the calcination at higher temperatures modifies the size of cobalt oxide crystals. The highest conversions on Co/Al-sg catalysts were over 90% (350–400°C) in dry and 66% (500°C) in wet gas mixture. Co/Al-ref had lower activity than Co/Al-sg after calcination at 600°C. The activities were the same as or higher with every CoO_x /alumina catalysts after calcination at 700 or 800°C than at 600°C. The Co/Al-sg with Al/Co of 650 initiated the propene oxidation at a 45°C lower temperature than Al-sg. This means that catalysts with low Co concentration had a high propene oxidation activity but also low NO oxidation and reduction abilities. Co addition on Al-2 did not change propene oxidation performance compared to Al-2. Co/Al-2 had a low activity, if the calcination temperature was as low as 600°C, because the propene oxidation activity of Al-2 itself was too high. Cobalt oxide has no essential part in oxidizing propene on these catalysts. Increasing temperature improved the conversion to nitrogen and the optimal calcination temperature coincided to 700°C. The differences between Co nitrate and acetate precursor on Al-2 were not so high as for Al-sg based catalysts.

The influence of calcination temperature between 600 and 1000°C and the precursor (nitrate or acetate) for Co/Al-sg were at first investigated using Al/Co ratio 65 in a dry NO–propene–oxygen mixture. The acetate precursor is preferable for CoO_x /alumina calcined at lower temperatures, where probably the nitrate species keep Co in a more inactive form. The raise of calcination temperature from 600 to 700°C markedly increased activities especially for CoO_x /alumina prepared from Co nitrate (nitrate ver-

sion). For the catalysts prepared from acetate precursor (acetate version) raising calcination temperature had less benefit. The slight increase in propene oxidation at 400–450°C on the nitrate version calcined at 700°C can be explained by the increased NO activity when NO reacted with propene. The catalysts calcined at 800°C had lost partly their activity.

When wet2 methods was used for impregnation, no change in activity was detected compared to a wet1-impregnated sample. Therefore, interaction between Co and Al oxides is not very sensitive to changes in impregnation.

Pure Co_3O_4 has presented high activity toward propene oxidation but a low ability to catalyze the NO reduction (Fig. 1). These results showed that the separate Co oxide phases formed at in higher calcination temperatures are more active than highly dispersed Co oxide particles formed on alumina at lower calcination temperatures.

The wide differences between Co catalysts calcined at 600 and 700°C was the reason to make experiments, where Al-sg was at first calcined at 700°C before Co impregnation (Fig. 1). This comparison revealed that on the sample (Co/Al-sg700(600)), where Co was impregnated on Al-sg(700), Co resulted probably in more inactive forms. As a result the NO reduction activity was lower on Co/Al-sg700(600) than on Co/Al-sg(600) and Co/Al-sg(700). Almost no change in propene oxidation activity was noticed. When the same procedure was made using Al-2, interesting results appeared. The propene oxidation activity of Co/Al-2/700(600) was even higher than on Al-2(600) but the NO reduction was practically diminished. This means that the initial activity of Al-2 calcined 600°C, was returned or there exists species like separate CoO_x particles, which also have a higher activity for propene oxidation. However, the detected HC oxidation activity resembles more that of Al-2 than coprecipitated CoO_x . The measured conversions can be explained by the co-operation of Al-2(700) and separate CoO_x particles (Co_3O_4).

The mechanical mixture of Co_3O_4 and Al-sg (Al/Co=65) showed a very high propene oxidation activity due to the high activity of Co_3O_4 particles, which caused a low NO reduction ability (maximum 39% at 300°C). Pure Al-sg (T_{50} =470°C for propene) and Co_3O_4 (T_{50} <200°C for propene) shows the upper and lower temperature limits for propene oxidation,

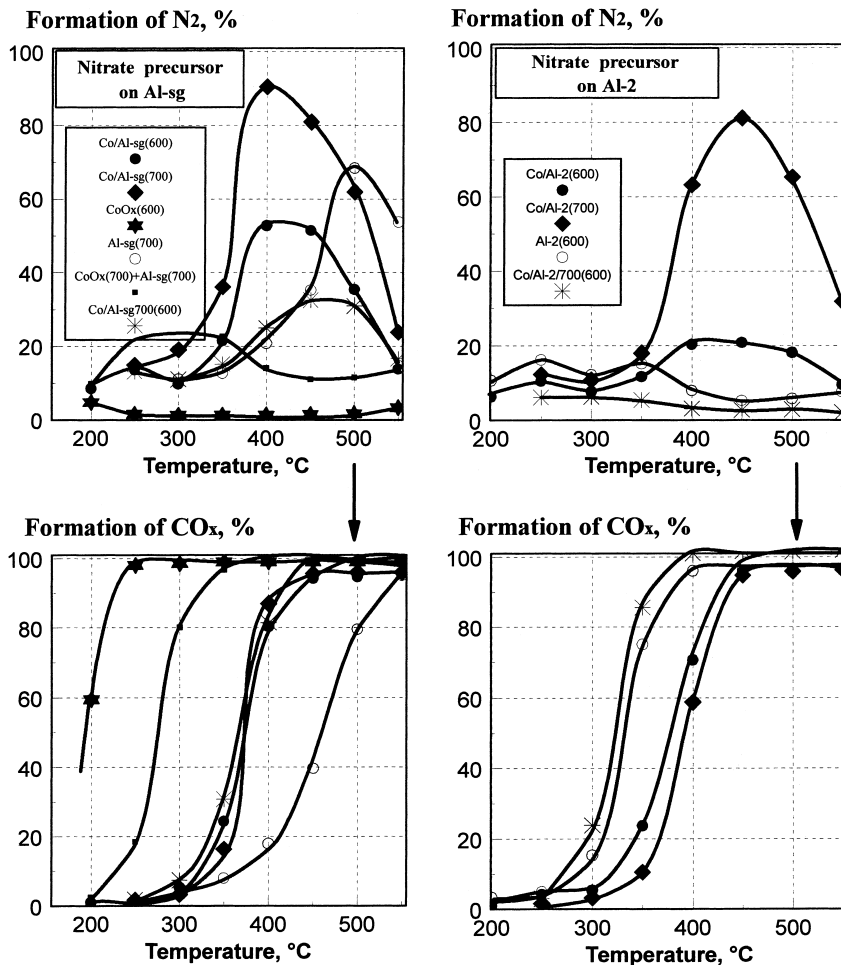


Fig. 1. Effect of preparation method on activity of $\text{CoO}_x/\text{alumina}$ catalysts ($\text{Al}/\text{Co}=65$; NO , 1000 ppm; C_3H_6 , 1000 ppm; O_2 , 10%; He balance, $F/W=20 \text{ dm}^3 \text{ g}^{-1} \text{ h}^{-1}$).

which is further connected to NO_x reduction window. Even if the contact points between Al-sg and CoO_x particles are very few in this mechanical mixture, relatively high activities were detected. Similar type of spillover of surface species or transfer by gaseous compounds is assumed in other cases [20]. In addition, reaction between these solid phases might happen slowly under these reaction conditions.

3.1.2. Optimization of the Al/Co ratio and calcination temperature of Co/Al-sg for $\text{NO}-\text{C}_3\text{H}_6-\text{O}_2$

When varying the Co loading between 0.2 and 5.5 wt.% ($\text{Al}/\text{Co}=650-20$) using calcination temperature of 700°C and Al-sg as support in dry and wet condition, the highest NO reduction by propene to nitrogen was observed with the loading of 0.8–1.8 wt.% Co (Table 2). The light-off performance was the

best when Al/Co ratio was 65 (1.8 wt.% Co). In dry conditions the highest activity was shifted to higher temperatures when the Co loading was decreased. These results suggest that in wet conditions higher Co loadings are preferable. The Co loading of 2.5 wt.% (Al/Co=45) was clearly too high on this alumina. On the highest Co loaded catalyst (Al/Co=20, 5.5 wt.% Co), separate Co oxide particles existed on Al-sg, which have a much higher activity to propene oxidation than Co species well dispersed on alumina.

According to two-variable (Co loading, calcination temperature) optimization for Co/Al-sg in dry conditions, the optimal Co loading was found to be between 130–45 (0.8–2.5 wt.%) of Al/Co, when the sample was calcined at 700°C. When Co loading was higher, it is preferable to calcinate the catalyst at higher temperatures, like 800°C. The calcination at higher temperature can compensate the increased HC oxidation activity caused by higher loading. The highest nitrogen formation was measured in the operation range of 400–450°C with Al/Co ratio of 100–200 calcined at 700–800°C. The contour graph for two-variable optimization as a function of temperature has been shown in Fig. 2. In fact, this was three variable optimization, where two (loading and calcination temperature) are related to preparation and one variable (operation temperature) is related to reaction conditions.

In the presence of water, the optimal Co loading was also 0.8–2.5 wt.%, but the operation window was shifted to higher temperatures, up to around 500°C. The maximum conversions were over 60% (Al/Co=65, calcined at 700°C). The contour presentation for the optimization of the activity in respect of Co loading and calcination temperature can be seen in Fig. 3. The reaction mechanism and kinetic equations presented in the next sections will show that the optimal parameters in preparation are connected to the compositions of exhaust gases and long-term durability.

3.1.3. Reactivities of nitrogen oxide and hydrocarbon species

When NO₂ was used instead of NO in feed gas, the reduction rate in the low temperature range was improved (Fig. 4). Co containing samples showed the same high activity as alumina-only catalysts, which evidences that the final NO reduction step occurred on

Al₂O₃ surface. In the presence of NO₂, less N₂O was formed, which confirmed that the last remaining N–O bond do not break off so easily in NO₂ than in NO. It is proposed for Pt/Al₂O₃ that nitrous oxide formation is preceded by adsorbate-assisted NO dissociation [21].

The highest formation of CO coincided with the highest increase of propene oxidation rate. The CO maximum formation was 9% with NO₂ at 400°C but 4.5% with NO at 350–400°C. Therefore, the ability of NO₂ to enhance the partial oxidation of propene was detected as CO in gas phase.

In addition, the NO reduction in the absence of oxygen and the N₂O reduction by propene in the presence of oxygen was investigated on CoO_x/alumina. The reduction rates were very low and HC light-off temperature was over 500°C. No differences were detected on Co/Al-sg and Co/Al-2 in respect of nitrate or acetate precursors. Al-sg had almost no activity for the rich side NO reduction but Al-2 showed higher activities in dry conditions even at lower temperatures. The reduction window on Al-2 was wide, which can be related to the higher conversion of propene to CO₂ and CO.

The results with the wet NO–propene–oxygen mixture showed the relationship between hydroxyl groups and moisture. As the surface property change caused by calcination are partly reversible, this effect is also related to the reaction mechanism. These experiments showed that the activity differences accomplished by different preparation methods remained also in wet conditions. The activity differences depend on the interactions between cobalt and alumina, where the formation of aluminates and different metal oxide species has a connection to the preparation method.

Different hydrocarbons were tried as reductants on Co/Al-sg(65) calcined at 700°C. The results showed that ethylene and propane are as good NO_x reductants as propene (Table 3). Methanol and ethanol had an operation window at lower temperatures (250–350°C). The N₂O formation is a problem with methanol. A reason is the high reactivity of methanol, which causes the initiation of the main reactions at temperatures where nitrous oxide formation is thermodynamically and kinetically probable. In the presence of water, CO formation was as high as 21% of C₃H₆ at 500°C. Methane and iso-propanol were poor reductants on CoO_x/alumina catalysts.

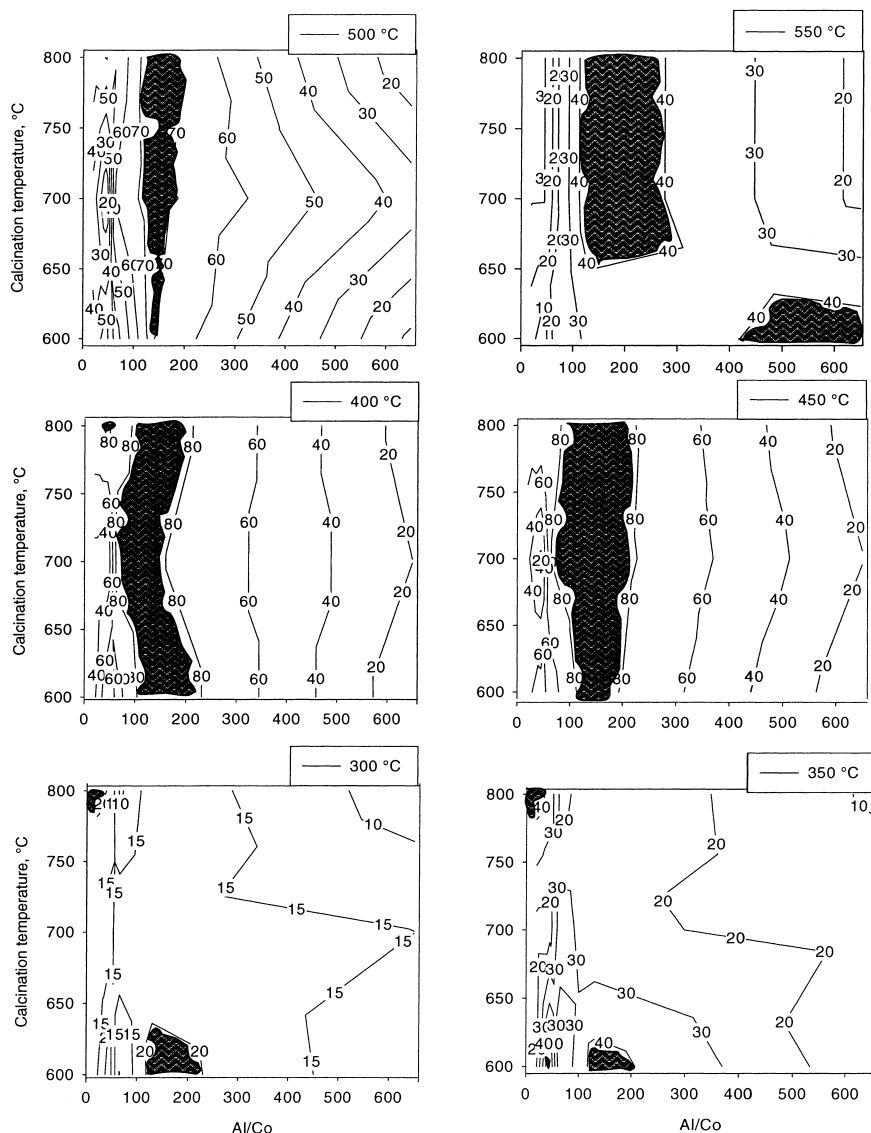


Fig. 2. Optimization of Co loading and calcination temperature by N₂ formation (%) in the absence of water at different operation temperatures (NO, 1000 ppm; C₃H₆, 1000 ppm; O₂, 10%; F/W=20 dm³ g⁻¹ h⁻¹). Optimum shadowed.

3.2. Catalyst characterization

3.2.1. BET

The surface area (BET) depends on Al/Co ratio and the calcination temperature (Table 1). Impregna-

tion with cobalt solution decreased surface area of Al-sg from the initial level of 300 m² g⁻¹ to the range of 194–224 m² g⁻¹. Hydrothermal collapse of original Al-sg in impregnation is assumed to be caused mainly by water itself, but ionic species (cobalt,

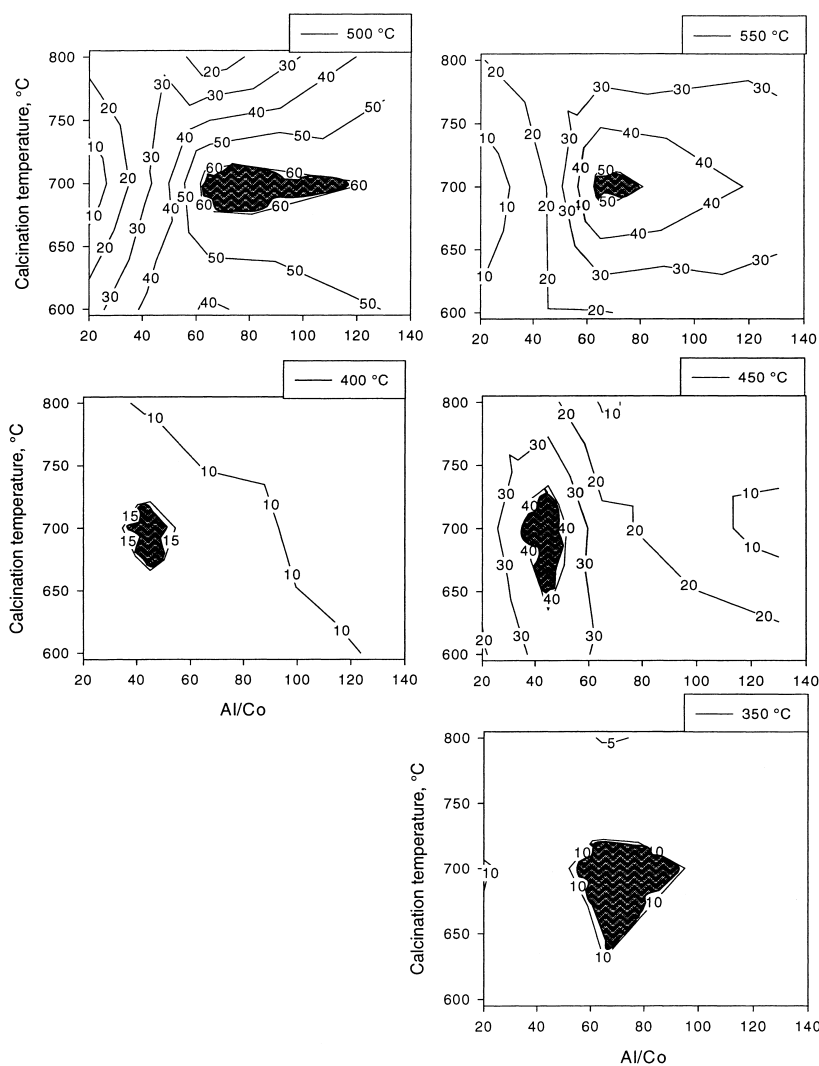


Fig. 3. Optimization of Co loading and calcination temperature by N₂ formation (%) in the presence of water at different operation temperatures (NO, 1000 ppm; C₃H₆, 1000 ppm; O₂, 10%; H₂O, 8%; F/W=20 dm³ g⁻¹ h⁻¹). Optimum shadowed.

nitrate and acetate) can accelerate the degradation. The resulting catalysts have a surface area on the typical level to γ -alumina prepared by conventional methods. Therefore, impregnation with aqueous solutions ruined partly the high surface area of alumina produced by sol-gel preparation. The catalysts prepared in water solutions continue the hydrothermal inter-

actions on alumina surface during thermal treatment, which alters the catalyst activity [22]. The surface area decreased as a function of increasing Co loading in the range of 0.2–5.5 wt.% and the calcination temperature in the range of 600–900 °C. But no direct connection between surface area and activities was found.

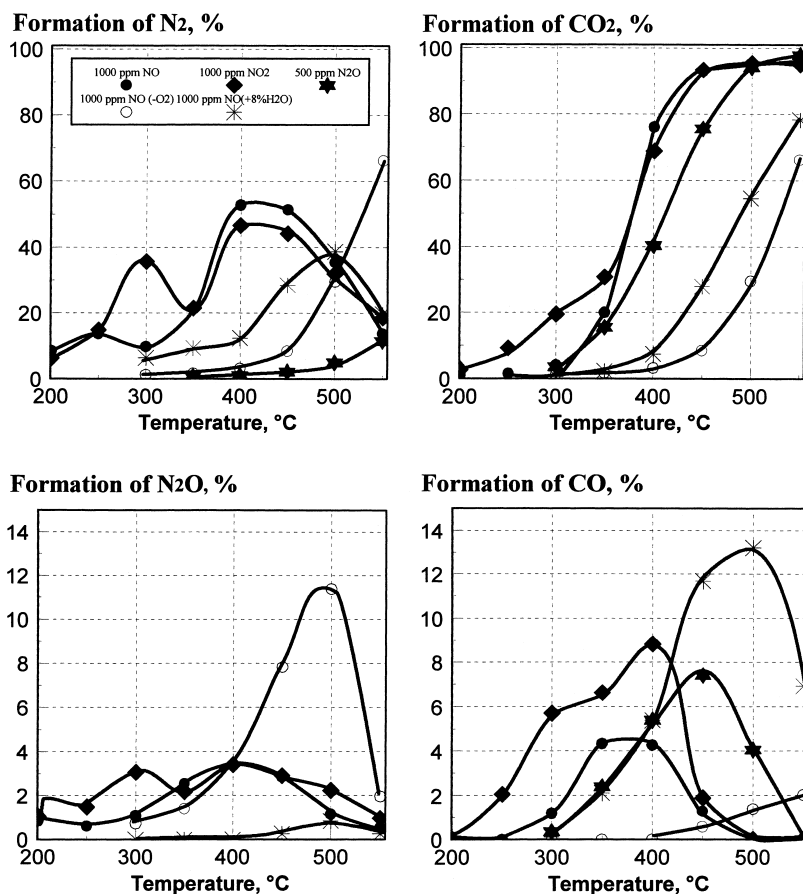


Fig. 4. Dependency of nitrogen oxide reduction on feed composition on Co/Al-sg (65,600) (C₃H₆, 1000 ppm; O₂, 10%, He balance, F/W=20 dm³ g⁻¹ h⁻¹).

3.2.2. XRD

XRD data for alumina catalysts showed that at 900 °C Al-sg has clearly transformed from γ - and δ -form to the direction of θ -alumina. No α -alumina was detected. An explanation for the high activities of Co/Al-sg(700) can be the observation that at 700 °C alumina phase is almost unchanged compared to the samples calcined at 600 °C, but at the same time the interaction between Co and Al oxides was converted in the direction of higher activities (Fig. 5). In addition to the former alumina forms, κ - and β -form can be formed in these conditions. The main shifts have a

logical correlation to the initial state and their thermal stability. The deviation factor of α -form is very low compared to activated γ -form alumina. Al-2 seemed to keep almost the same phase structure up to 900 °C and so the original δ -alumina is stable up to that temperature. Co containing samples were more complicated to analyze, because both Al and Co oxides had a possibility to be modified during thermal treatments and it was difficult to detect Co species on Co/Al-sg with as low a Co loading as 1.8 wt.%, which showed the highest activity. Detectable Co₃O₄ is evidently as larger particles, too. It is assumed that CoAl₂O₄ (Co

Table 3

The efficiency of different hydrocarbons for the NO_x reduction over Co/Al-sg(65,700)^a

Reductant	Maximum product formations			Oxidation of reductant T ₅₀ , (°C)
	Formation-%, dry/wet			
	N ₂ (at T, °C)	N ₂ O	CO	
C ₃ H ₆	91(400)/66(500)	3/1	5/21	375/455
C ₃ H ₈	79(500)/–	2/–	3/–	450/–
C ₂ H ₄	73(450)/–	3/–	3/–	415/–
CH ₄	8(550)/–	1/–	–/–	510/–
MeOH	31(300)/24(300)	14/11	11/10	280/295
EtOH	30(300)/–	3/–	8/–	310/–
<i>i</i> -PrOH	23(500)/11(550)	2/0.5	5/6	330/345

^a 1000 ppm NO; 10% O₂; 0 or 8% H₂O; C₃H₆=C₃H₈=C₂H₄=CH₄=MeOH=1000 ppm and EtOH=*i*-PrOH=400 ppm; balance He, F/W=20 dm³ g⁻¹ h⁻¹.

aluminate) might be formed on the sample calcined at 900°C, but the peaks of Co₃O₄ and Co aluminate are overlapping heavily in the same range. The γ-alumina structure degradation was also detected on Co/Al-sg calcined at 900°C. When increasing the Co concentration up to 5.5 wt.% on the sample calcined at 600°C, Co₃O₄ peaks became stronger. This gives an explanation for the results in activity evaluations, because larger Co₃O₄ clusters are too active for propene oxidation. It has been proposed that when the Co loading is moderate and CoO_x/alumina is treated at higher temperatures to redisperse Co²⁺ on Al₂O₃, formed

CoO on alumina surface is improving the efficiency of the catalysts [15].

3.2.3. TGA

The purpose of thermogravimetric analysis was to confirm the stability of cobalt catalysts. The possible forms of cobalt on alumina are Co₃O₄, CoO, Co and Co aluminate. The reference sample Co₃O₄ (CoO_{1.33}) decomposed partly between 927 and 974°C losing in this sharp TG transformation about 7% of the weight, the weight loss which represents the transformation from Co₃O₄ to CoO, but on Co/Al-sg(65,600) no

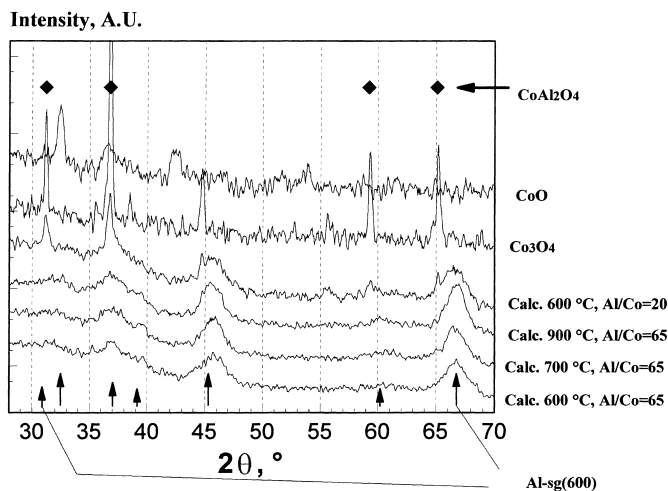


Fig. 5. Phase analysis of Co/Al-sg by XRD. Effect of calcination temperature and Al/Co.

transformation was detected. Even if the amount of cobalt is as low as 1.8 wt.% in sample, sharper changes should be noticed. Alumina support can stabilize Co to keep the higher oxidation state as pure Co_3O_4 . Probably higher valences of cobalt would be observed if the lower calcination temperatures like 400–500°C or higher Co loading were used but from the practical point of view low calcination temperatures are not interesting. According to these TGA it is not possible to decide if Co is in the form of Co_3O_4 , CoO or Co aluminate.

3.2.4. XPS

The state of Co species was detected by binding energies of Co $2p_{3/2}$ (Table 4). Cobalt on δ -Al-2 after calcination at 600°C was the nearest to Co_3O_4 than on any other samples, the observation of which explained the performance similarities of Co/Al-2 and Co_3O_4 . Co^{2+} was clearly the main phase on Co/Al-sg calcined at 600°C. In addition, the satellite peaks detected on different Co/Al-sg samples indicated the presence of Co^{2+} instead of Co_3O_4 . The activation of Co/Al-sg by calcination at 700°C was seen by the binding energy shift between the samples calcined at 600 and 700°C. The catalysts with the highest activities had the binding energies around 781.4 eV. It was not possible to estimate the surface Co/Al ratio quantitatively by XPS measurements. As the binding energy of Co aluminate and Co^{2+} is the same, it was not possible to make a difference between these species by main peaks. Therefore, depending on the Al/Co and the treatments, CoO_x /alumina catalysts contain Co_3O_4 , Co^{2+} incorporated in aluminum oxide lattice in CoAl_2O_4 and dis-

persed Co^{2+} on alumina surface. According to NMR studies the coordination of Co (tetrahedral and octahedral) has a significant role in activation of NO reduction reactions [15]. It is assumed that coordination of Co^{2+} species is the key issue to explain the activities.

3.3. Reaction intermediates

FTIR spectra were recorded over Co/Al-sg(65,700) in the presence of pure NO, C_3H_6 or O_2 at 26 mbar or the same species as adsorbed on the evacuated surface at 50, 150, 250 and 350°C (Fig. 6). The single gas experiments with Co/Al-sg and Al-sg verified that no molecular nitrogen adsorbed on these catalysts. The reason for this measurement was the fact that inert gases like nitrogen can cause collision assisted desorptions to happen or adsorb physically with low partial pressures as detectable FTIR peaks on catalyst surface. In single gas experiments no CO or N_2O adsorption on Al-sg was detected at 150°C but these compounds were activated at 350°C (CO 1589 and 1396 cm^{-1} ; N_2O 2233, 2210, 1580, 1528, 1304 and 1269 cm^{-1}). Nitrates (1225–1230 cm^{-1}) on alumina surface were detected up to 250°C on Al-sg and Co/Al-sg. NO adsorption at 350°C resulted in the bands of 2270–2230, 1527 and 1400 cm^{-1} on Al-sg and 2308, 2305, 2226 and 1238 cm^{-1} on Co/Al-sg. NO adsorption (1801 and 1880 cm^{-1}) on Co surface was detected clearly at 50°C. Propene caused the peaks of 1485, 1574, 1400 cm^{-1} on Al-sg and 1587, 1452, 1389 and 2359 cm^{-1} on Co/Al-sg at 350°C. No match with the adsorption bands caused by methane was found. Strong adsorption of CO_2 was detected at

Table 4
XPS binding energies for the cobalt samples (eV)

Sample (T_{calc} , precursor)	Co $2p_{3/2}$	O 1s	Al 2p
Co/Al-sg (600, nitr)	781.8	531.4	74.5
Co/Al-sg (700, nitr)	781.5	531.3	74.4
Co/Al-sg (1000, nitr)	781.4	531.1	74.2
Co/Al-sg (600, acet)	781.6	531.2	74.4
Co/Al-2 (600, nitr)	781.2	531.3	74.4
Co/Al-2 (700, nitr)	781.4	531.4	74.5
References ^a			
Co_3O_4	780.2	529.9	–
Co(acac) ₂	782.0	–	–
CoAl_2O_4	782.0	–	–

^a C 1s=285.0 eV chemical shift reference.

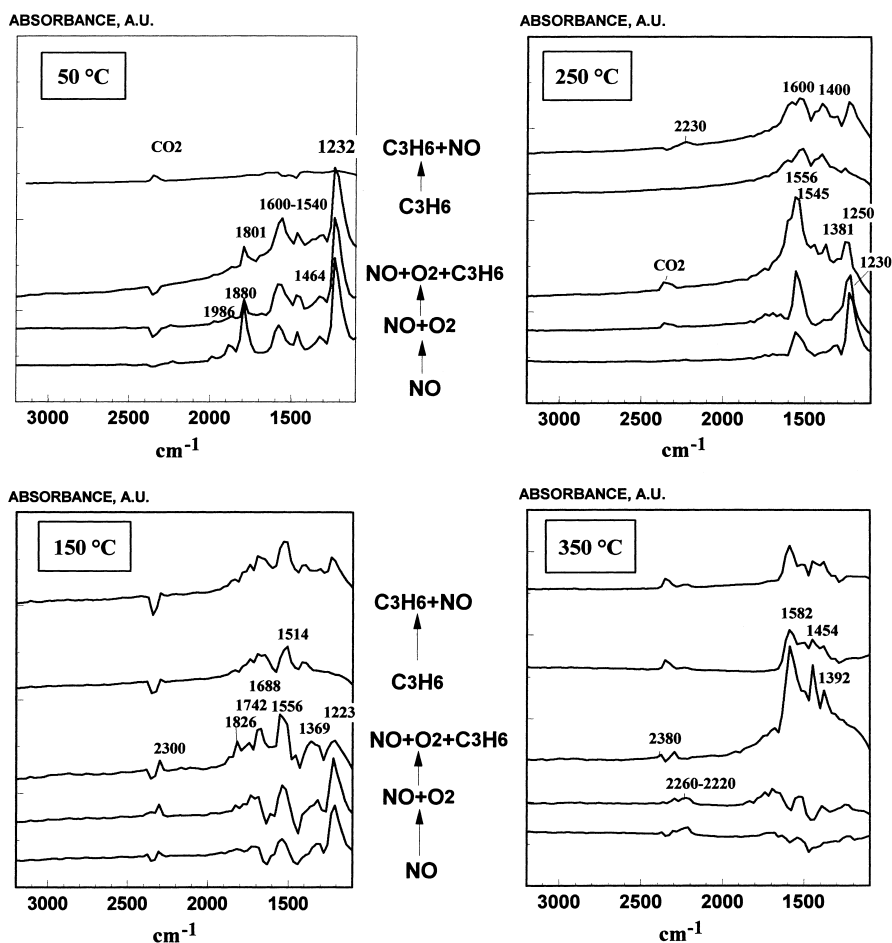


Fig. 6. FTIR spectra on Co/Al-sg(65,700; nitrogen) after the introduction of NO, C₃H₆ and O₂ and evacuation at different temperatures.

150 °C by the bands of 2314, 1651, 1520, 1435 and 1227 cm⁻¹ but the peaks of 2318 and 1516 cm⁻¹ were left at 350 °C on Al-sg. At lower temperatures NO compounds but at higher temperatures (≥ 350 °C) hydrocarbon species mainly covered the surface and the preadsorption of NO+O₂ enhanced the partial oxidation of propene on Co/Al-sg. The addition of propene on this surface caused the intense peaks of 1582, 1454 and 1392 cm⁻¹ (hydrogen-carbon-oxygen compounds) at 350 °C. The spectra mostly resembled that of propene single adsorption on Co/Al-sg with the

addition that NCO or possibly CN group containing compounds were also detected. However, Ukisu et al. [23,24] found that isocyanate formation is suppressed in the presence of water. The stability of HNCO is limited to very low temperatures. As adsorption of ammonia or ammonium on metal oxide catalysts has been observed in the range of 1400–1480 cm⁻¹ [25,26], the intermediates containing N–H bond are not excluded in our later assumptions.

It has been detected in other studies that when Co concentration is under 2 wt.% on alumina, Co ions are

located on octahedral alumina vacancies and spectra are similar to NO adsorption on Co aluminate [27]. In the case of higher Co loading, adsorption is similar to NO on Co_3O_4 and with lower loading, adsorption is similar to NO on isolated Co^{2+} . Also the pretreatment at higher temperatures increases NO adsorption capacities on Co aluminate or on cobalt located on octahedral sites [28].

NO has a tendency to adsorb in pairs on transition metal oxides, which has been ascribed to the fact that two adsorbed NO molecules are stabilized by mutual interaction [26,29]. In some other studies adsorbed N_2O_4 species ($1250\text{--}1350\text{ cm}^{-1}$) existed on catalyst surface [30]. Linearly bonded NO species are detected by FTIR in the wavelength range of $>1850\text{ cm}^{-1}$. The disproportionation of NO is assumed to take place by the formation of N_2O_2 (* denotes surface active sites):



Our observations did not confirm these proposals, because N_2O and NO_2 formation has been detected in the different conditions and usually the adsorption of any nitrogen species was detected at temperatures clearly below the reaction temperature. In the presence of a high concentration of NO_2 , N_2O_4 dimers can also exist in exhaust gas or on catalyst surface. Even if we did not include these intermediates in our reaction mechanism, the existence of this type of compounds supports our proposal, where the final N–N bond formation proceeds by the reaction of NO and carbon–hydrogen containing surface species. When two nitrogen atoms, as in N_2O_4 or N_2O_2 , are located on the molecular scale vicinity to partially oxidized hydrocarbon species, the probability for dinitrogen formation by our proposed mechanism is higher than in the presence of separate NO molecules. In that case the other nitrogen atom should be first attached with hydrogen, carbon or both. Many catalyst and gas phase studies support the proposal that NO_2 is more reactive in adding oxygen to carbon and NO more reactive in forming NCO or CN compounds [31,32].

A variety of intermediates was detected in FTIR studies on Co/Al-sg under different reaction conditions, which were simplified compared to really occurring conditions. We were not able to assign all the peaks exactly but a part of the peaks were explained in general level by the type of compounds usually

detected on that wavelength. In particular, in the reaction where hydrocarbons are involved, the number of probable parallel and sequential reactions is huge. Therefore, it is difficult to propose and take account into quantitative kinetic modeling all the single reaction possible in the prevailing conditions. According to the review of Matyshak and Krylov [33], even the detections for the first step in propene adsorption are various and they can be described by our denotations as $\text{C}_3\text{H}_4\text{O}^*$, C_3H_6^* , $\text{C}_3\text{H}_6\text{O}^*$, $\text{C}_3\text{H}_7\text{O}^*$ or $\text{C}_3\text{H}_7\text{OH}^*$. In fact, the balance between surface O^{2-} and OH^- is so sensitive and reversible in the usual reaction conditions that they can not be easily detected in situ but can be considered in general level. The presence of OH groups in active sites could balance the amount of hydrogen atoms to the right level, if C=C bond was changed to C–C bond in formation of partially oxidized propene ($\text{C}_3\text{H}_7\text{O}^*$). We propose $\text{C}_3\text{H}_6\text{O}^*$ as an initial compound for catalytic propene reactions. This molecule formula can be described by the formation of C=O bonding on $\text{CoO}_x/\text{alumina}$ surface, if C=C bond is changed to C–C bond ($\text{CH}_3\text{--CH}_2\text{--HC=O}$). The difference between the results on unsaturated, saturated, and oxygenated hydrocarbons was an evidence supporting the description in our reaction mechanism proposal concerning the functional groups of C=C, C=O and C–OH.

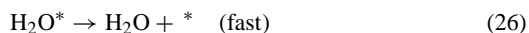
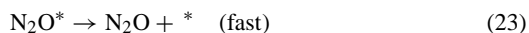
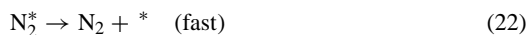
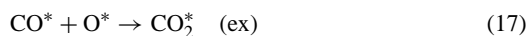
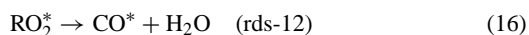
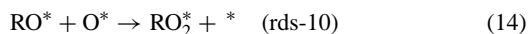
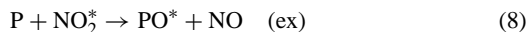
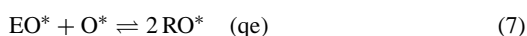
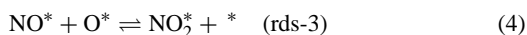
The observations with FTIR showed the existence of H–C–O compounds at higher temperatures and the existence of NCO and possibly CN groups, when NO was present in propene–oxygen system. The enhancement of $\text{NO}+\text{O}_2$ and NO_2 for the formation of partially oxidized hydrocarbons was detected at the temperatures above 350°C . The fact that high amount of nitrates are present only at low temperatures focus us to consider other routes than the nitrate route for the NO reduction by propene. When the reaction is really proceeding, no nitrates are found on surface but totally different types of intermediates. Often FTIR experiments are made at low or room temperature but these types of studies show the surface coverages when no reactions are proceeding on catalysts and usually the detected compounds are the main reason for the inhibition against the initiation of reactions. Our experiments tried to cover the temperatures up to the reaction temperatures found by activity experiments. The observations at the highest temperatures are the most critical for reaction mechanism assumptions. In

general, the activation of the reductant is the rate determining step in NO reduction reactions.

3.4. Reaction mechanism

Based on observations in activity and surface studies, the next assumptions have been made for reaction mechanism. The reaction pathways have proposed in such a way that hydrogen and carbon are staying in intermediates up to the point when a C₁ compound and nitrogen from NO is formed. Thus, we can fix the intermediates and separate the atom balance in the simplest way to interpret the reaction kinetics. In fact the paths to different C₁ compounds are various. In reality a part of hydrogen and carbon are lost for water and CO_x formation before the final nitrogen formation. Another reason is that adsorbed oxygenated hydrocarbon intermediates are detected by FTIR studies. It has been noticed in many experiments that NO₂ has a significant oxidant for hydrocarbon oxidation. In the case of a high temperature deNO_x catalyst, a N₂O intermediate is not an important route for nitrogen. The catalyst has at least two type of active centers (Al and Co sites) but for simplicity and because of the fact that both of them can take part at the same time in many reaction steps and the intimate contact of sites is necessary, we are proposing in kinetic calculations that the catalyst is containing only one active site: CoAl site. In practice, the active site is defined by our characterization studies to finely dispersed Co²⁺ in aluminum oxide.

Many reaction pathways are prevailing at the same time but this kind of reaction mechanism is common enough to interpret the kinetic limitations and show dynamics in catalytic reactions, where many serial and parallel reactions are simultaneously proceeding. Based on these assumptions the reaction mechanism is proposed by the following way:



where P=C₃H₆; E=C₂H₄; R=CH₂; qe=quasi-equilibrium; rds=rate determining step-nr, related to *k_{nr}* in model; fast=extremely fast reaction; ex=excluded in model.

The final reductant intermediate, NRO, is in our proposal exactly specified to H₂NCO. These type of intermediates are very plausible reductants to form N–N bonding (compare to the selective catalytic reduction of NO with NH₃). In a recent study with CH₄+NO on Co/ZSM-5, similar type of final intermediate (formamide, H₂NCOH) was proposed [34]. The bond order can be changed by Beckmann arrangement, where the oxygen atom attached to nitrogen is moved to carbon leading to the formation of nitrite and carboxyl groups. NO bond was broken in the formation of NRO species. Many other type of nitrogen containing intermediates, containing more than one carbon atom

and the formation of N–N bond by bond rearrangements within the same molecules have been proposed to have crucial part in NO_x reduction [35–37]. We assume that detected nitro group containing hydrocarbons can have a role in activation of propene to form PO* but they are not the final compounds preceding N₂ formation. In principle, the compounds consisting of C–N or N–H bonding attached to the hydrocarbon chain containing more than one carbon atom, are plausible candidates to form N–N bonding but as a surface reaction that route is more probable on zeolite based than on metal oxide based catalysts. Surface concentrations of hydrocarbon species are much higher on zeolites than on metal oxides in catalytic reactions.

Even if the most experiments were done without water in feed, the negative effect of water can be explained by the reaction mechanism, if the Eq. (26) is proposed to be quasi-equilibrium reaction. The increase in partial pressure of water in gas phase causes higher H₂O coverage suppressing the formation of CO_x. The promoting effect of oxygen is evident to initiate oxidation and remove unburned compounds from surface. In addition, the reaction sequence initiation is enhanced when NO₂ is formed. The proposed reaction sequence is as well valid to explain the formation and NO_x reduction ability of ethylene and methane. Based on the reaction mechanism it is very difficult to reduce NO by methane. However, catalytic methane oxidation reactions should have other initiation steps excluded in our simplified mechanism. The reaction of oxygenates like alcohols can be understood by the easier adsorption of PO*, EO*, RO* or RO₂* on surface.

3.5. Kinetic model

Reaction steps with a notation of ex were neglected in the kinetic model and steps which were marked fast was proposed to be so extremely fast that left hand side reactants virtually do not exist in the surface. The assistance of NO₂ in partial oxidation steps were excluded for model simplicity. Asymptotical correctness of the reaction rate equations, when one of the oxidants O₂, NO or NO₂ do not exist in gas phase, requires that NO₂ is an additional, not primary, route in partial oxidation. The quasi-equilibrium approximation was applied to the steps with notation of qe

to calculate equilibrium constants (K_i):

$$K_{\text{NO}} = \frac{\theta_{\text{NO}}}{c_{\text{NO}}\theta_v} \quad (27)$$

$$K_{\text{O}_2} = \frac{\theta_{\text{O}}^2}{c_{\text{O}_2}\theta_v^2} \quad (28)$$

$$K_{\text{P}} = \frac{\theta_{\text{PO}}}{c_{\text{P}}\theta_{\text{O}}} \quad (29)$$

$$K_{\text{E}} = \frac{\theta_{\text{EO}}\theta_{\text{RO}}}{\theta_{\text{PO}}\theta_{\text{O}}} \quad (30)$$

$$K_{\text{R}} = \frac{\theta_{\text{RO}}^2}{\theta_{\text{EO}}\theta_{\text{O}}} \quad (31)$$

$$K_{\text{NRO}} = \frac{\theta_{\text{NRO}}\theta_{\text{O}}}{\theta_{\text{RO}}\theta_{\text{NO}}} \quad (32)$$

$$K_{\text{CO}} = \frac{\theta_{\text{CO}}}{c_{\text{CO}}\theta_v} \quad (33)$$

$$K_{\text{NO}_2} = \frac{\theta_{\text{NO}_2}}{c_{\text{NO}_2}\theta_v} \quad (34)$$

For the rate determining steps the rate equations can be written based on law of mass action. For the surface coverage (θ_i) the site balance is

$$\theta_v + \theta_{\text{PO}} + \theta_{\text{EO}} + \theta_{\text{RO}} + \theta_{\text{RO}_2} + \theta_{\text{CO}} + \theta_{\text{NRO}} + \theta_{\text{O}} + \theta_{\text{NO}} + \theta_{\text{NO}_2} = 1 \quad (35)$$

The application of the quasi-equilibrium, steady-state hypothesis of RO₂* surface complex coverage and rate equations of the rate determining steps gives the unknown surface coverages. For the vacant sites it is given

$$\begin{aligned} \frac{1}{\theta_v} = & K_{\text{P}}^{1/3} K_{\text{E}}^{1/3} K_{\text{R}}^{1/3} K_{\text{O}_2}^{1/2} c_{\text{P}}^{1/3} c_{\text{O}_2}^{1/2} + K_{\text{P}}^{2/3} K_{\text{E}}^{2/3} \\ & \times K_{\text{R}}^{-1/3} K_{\text{O}_2}^{1/2} c_{\text{P}}^{2/3} c_{\text{O}_2}^{1/2} + K_{\text{P}} K_{\text{O}_2}^{1/2} c_{\text{P}} c_{\text{O}_2}^{1/2} \\ & + k_8 k_{11}^{-1} K_{\text{NRO}} K_{\text{P}}^{1/3} K_{\text{E}}^{1/3} K_{\text{R}}^{1/3} K_{\text{NO}}^2 K_{\text{O}_2}^{-1/2} c_{\text{P}}^{1/3} \\ & \times c_{\text{NO}}^2 c_{\text{O}_2}^{-1/2} + K_{\text{CO}} c_{\text{CO}} + K_{\text{O}_2}^{1/2} c_{\text{O}_2}^{1/2} \\ & + k_{10} k_{11}^{-1} K_{\text{P}}^{1/3} K_{\text{E}}^{1/3} K_{\text{R}}^{1/3} K_{\text{O}_2}^{1/2} c_{\text{P}}^{1/3} c_{\text{O}_2}^{1/2} \\ & + K_{\text{NRO}} K_{\text{P}}^{1/3} K_{\text{E}}^{1/3} K_{\text{R}}^{1/3} K_{\text{NO}} c_{\text{P}}^{1/3} c_{\text{NO}} + K_{\text{NO}} c_{\text{NO}} \\ & + K_{\text{NO}_2} c_{\text{NO}_2} = D \end{aligned} \quad (36)$$

The steady-state rate equations are obtained for the rate determining step

$$r_3 = k_3 \left(\frac{K_{\text{NO}} K_{\text{O}_2}^{1/2} c_{\text{NO}} c_{\text{O}_2}^{1/2}}{D^2} - \frac{(1/K_{3\text{eq}}) K_{\text{NO}_2} c_{\text{NO}_2}}{D} \right) \quad (37)$$

$$r_8 = \frac{k_8 K_{\text{NRO}} K_{\text{P}}^{1/3} K_{\text{E}}^{1/3} K_{\text{R}}^{1/3} K_{\text{NO}}^2 c_{\text{P}}^{1/3} c_{\text{NO}}^2}{D^2} \quad (38)$$

$$r_9 = k_9 k_8^{-1} r_8 \quad (39)$$

$$r_{10} = \frac{k_{10} K_{\text{P}}^{1/3} K_{\text{E}}^{1/3} K_{\text{R}}^{1/3} K_{\text{O}_2} c_{\text{P}} c_{\text{O}_2}}{D^2} \quad (40)$$

$$r_{11} = r_8 + r_{10} \quad (41)$$

$$r_{12} = \frac{k_{12} K_{\text{P}}^{1/3} K_{\text{E}}^{1/3} K_{\text{R}}^{1/3} K_{\text{O}_2} c_{\text{P}}^{1/3} c_{\text{O}_2}}{D} \quad (42)$$

The generation rates of components ([compound]=molar concentration) are obtained from the rates (r_i) of rate determining steps and atom balances

$$\frac{d[\text{NO}]}{dt} = -2r_8 - 2r_9 - r_3 \quad (43)$$

$$\frac{d[\text{N}_2]}{dt} = r_8 \quad (44)$$

$$\frac{d[\text{CO}]}{dt} = r_{12} \quad (45)$$

$$\frac{d[\text{CO}_2]}{dt} = r_{11} \quad (46)$$

$$\frac{d[\text{NO}]}{dt} = r_9 \quad (47)$$

$$\frac{d[\text{P}]}{dt} = -\frac{1}{3} r_{11} - \frac{1}{3} r_{12} \quad (48)$$

$$\frac{d[\text{NO}_2]}{dt} = r_3 \quad (49)$$

$$\frac{d[\text{O}_2]}{dt} = \frac{3}{2} r_{11} + r_8 + \frac{1}{2} r_9 - \frac{1}{2} r_3 - r_{12} \quad (50)$$

$$\frac{d[\text{H}_2\text{O}]}{dt} = r_{11} + r_{12} \quad (51)$$

The reactor was described by a one-dimensional pseudo-homogeneous model. A plug-flow model without pressure drop was applied for gas phase. The catalytic reactor was assumed to operate in isothermal steady-state conditions. The surface was assumed to

be uniform with delocalized active sites. The following mass balance equation can be written for the gas phase

$$\frac{d\mathbf{y}}{dz} = \frac{m_{\text{cat}}}{\dot{n}} \mathbf{r} \quad (52)$$

where \mathbf{y} is the vector of mole fractions, z is a dimensionless length coordinate, m_{cat} is the mass of catalyst, \dot{n} is the total mole flow and \mathbf{r} is the generation rate vector of components. The system of ordinary differential equations was integrated numerically by backward difference method. The parameters were estimated by non-linear regression analysis optimized by simplex and Levenberg–Marquardt algorithms. The values of estimated parameters are shown in Table 5. A tight minimum was obtained for parameter k_3 but a clear maximum boundary does not exist. In that reason its temperature dependence is also unclear and it is proposed to be temperature independent, i.e., activation energy E_3 was given the value zero. All other parameters are well identified. A slightly better fit can be achieved, if activation energy E_{12} was floated to

Table 5
The estimated kinetic parameters for NO reduction by propene presence of oxygen

Parameter ^a	Value
K_{P}	$3.2 \times 10^{-3} \text{ m}^3 \text{ mol}^{-1}$
K_{E}	6.7
K_{R}	83
K_{NO}	$1.8 \text{ m}^3 \text{ mol}^{-1}$
K_{O_2}	$2.9 \times 10^{-7} \text{ m}^{3/2} \text{ mol}^{-1/2}$
K_{NRO}	8.6×10^{-4}
K_{CO}	$0 \text{ m}^3 \text{ mol}^{-1}$
K_{NO_2}	$1.1 \times 10^{-4} \text{ m}^3 \text{ mol}^{-1}$
k_3	4400
E_3	0 kJ mol^{-1}
K_3	1.9×10^{-2}
k_8	$6.6 \text{ mol kg}^{-1} \text{ s}^{-1}$
E_8	62 kJ mol^{-1}
k_9	$0.13 \text{ mol kg}^{-1} \text{ s}^{-1}$
E_9	63 kJ mol^{-1}
k_{10}	$8.3 \text{ mol kg}^{-1} \text{ s}^{-1}$
E_{10}	105 kJ mol^{-1}
k_{11}	$2.7 \times 10^{-3} \text{ mol kg}^{-1} \text{ s}^{-1}$
E_{11}	197 kJ mol^{-1}
k_{12}	$13.5 \text{ mol kg}^{-1} \text{ s}^{-1}$
E_{12}	0 kJ mol^{-1}

^a k_i : mean temperature (350°C) reaction rate constants; K_i : equilibrium constants; E_i : activation energy.

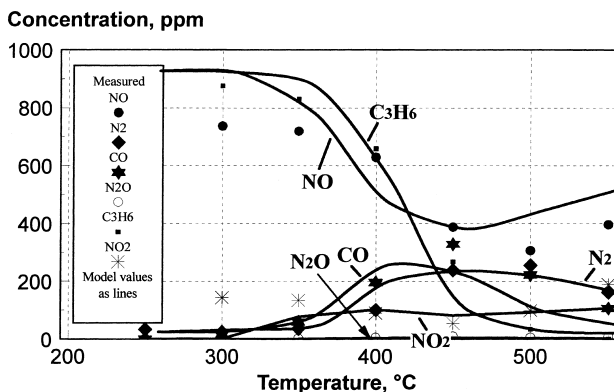


Fig. 7. Outlet concentrations by measurements and kinetic model on Co/Al-sg (Inlet: 1000 ppm NO, 1000 ppm C₃H₆, 10% O₂, $F/W=60 \text{ dm}^3 \text{ g}^{-1} \text{ h}^{-1}$).

a negative value, but that was not permitted, even if lumping effects could explain that.

An example in usual conditions shows the matching between the measured and modeled concentrations (Fig. 7). The formation of nitrogen and propene oxidation was explained well. In general, the worst prediction was calculated for CO and according to our model NO₂ concentration should be lower at low temperatures. Homogenous NO oxidation to NO₂ can explain the difference. The main gas concentrations

and surface coverages along the reactor length were simulated at 400 and 500°C (Fig. 8). Slow propene oxidation initiation by PO* allows NO to react through surface intermediates (NRO, NO) to nitrogen at 400°C. Propene oxidation proceeds very quickly at 500°C limiting NO reduction to nitrogen. In fact, the last part of reactor was useless to reduce NO in these conditions. The simulation can describe with good way most of the surface coverages expected by reaction mechanism. The kinetic model is according to our

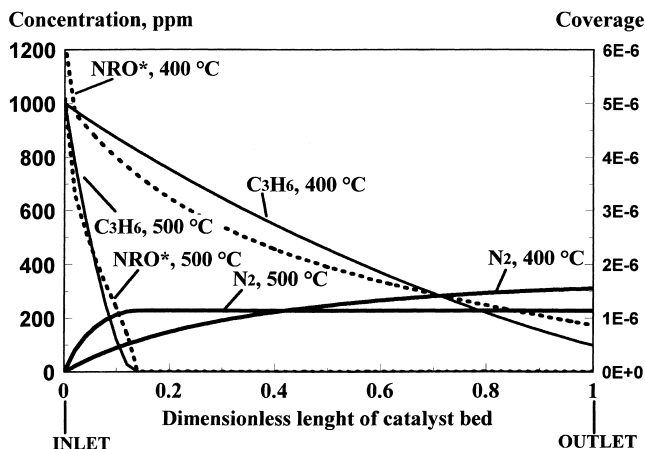


Fig. 8. Simulated gas phase concentrations and surface coverages along the length of Co/Al-sg catalyst bed at 400 and 500°C (Inlet: 1000 ppm NO, 1000 ppm C₃H₆, 10% O₂, $20 \text{ dm}^3 \text{ g}^{-1} \text{ h}^{-1}$). NRO* shown by dotted lines.

sensitivity analysis in the border by the extent, where all parameters are still statistically significant. The fluctuation in surface species coverages gives an excellent tool to understand and forecast the performance and limiting steps in NO_x reduction by propene.

4. Conclusions

The preparation method of CoO_x/alumina for NO_x reduction by propene in lean conditions was optimized with respect to the calcination temperature and the Co loading. The Co/Al-sg catalysts prepared by usual incipient wetness method showed the highest activities in the absence of water when the calcination temperature was 700–800°C and the loading in the range of 0.5–1.2 wt.%. In the presence of water the optimum was shifted to higher Co loadings (1.5–2.0 wt.%) and to the calcination temperatures of 680–700°C. In fact, the optimum is also dependent on the reactant concentrations.

Co₃O₄ and Co²⁺ species were observed on the active catalysts by XRD and XPS. Adsorption of nitrate and carbonate type surface compounds were detected at lower temperatures (≤250°C) on Co/Al-sg. Catalytically formed NO₂ enhanced the oxidation of propene to oxygenated hydrocarbons on CoO_x/alumina at higher temperatures (≥250°C). In the same temperature range, compounds containing nitrogen–carbon–hydrogen bonds were detected by in situ FTIR studies and nitrogen is formed from NO in the presence of propene and oxygen by activity experiments under the same conditions.

Reaction engineering approach was used to tie catalyst activity, characterization and surface species detections to a kinetic model, which explains the rate determining steps, the disappearance of reactants and the formation of all gaseous products in reactor outlet usually detected (N₂, N₂O, NO₂, CO, CO₂, C₂H₄, CH₄). The mechanistic kinetic model presented for a tubular catalyst reactor and the multivariable model for catalyst preparation are convenient tools to design the optimal catalytic reactor and predict reaction dynamics for NO_x reduction by hydrocarbons. We assume that the same model can be used to explain most of the results with other oxide based catalysts able to catalyze NO_x reduction by hydrocarbons in the high temperature deNO_x range [38].

Acknowledgements

The experiments in this study were carried out in a visiting researcher program funded by a fellowship from AIST. In addition to this the authors are grateful to the Cosmo Oil R&D Center for carrying out the XPS analysis.

References

- [1] H. Hamada, Y. Kintaichi, M. Sasaki, T. Ito, *Chem. Lett. Jpn.* (1990) 1069.
- [2] P.W. Park, J.K. Kil, H.H. Kung, M.C. Kung, *Catal. Today* 42 (1998) 51.
- [3] H. Hamada, Y. Kintaichi, T. Yoshinari, M. Tabata, M. Sasaki, T. Ito, *Catal. Today* 17 (1993) 111.
- [4] T. Miyadera, *Appl. Catal.* 2 (1993) 199.
- [5] R. Burch, P.J. Millington, A.P. Walker, *Appl. Catal. B* 4 (1994) 65.
- [6] Y. Teraoka, T. Harada, T. Iwasaki, T. Ikeda, S. Kagawa, *Jpn. Chem. Lett.* 5 (1993) 773.
- [7] G. Centi, S. Perathiner, *Appl. Catal. A* 132 (1995) 179.
- [8] M. Tabata, H. Hamada, F. Suganuma, T. Yoshinari, H. Tsuchida, Y. Kintaichi, M. Sasaki, T. Ito, *Catal. Lett.* 25 (1994) 55.
- [9] A. Ueda, T. Oshima, M. Haruta, *Appl. Catal. B* 12 (1997) 81.
- [10] H. Hamada, Y. Kintaichi, M. Sasaki, T. Ito, *Appl. Catal.* 75 (1991) L1.
- [11] H. Hamada, Y. Kintaichi, M. Tabata, M. Sasaki, T. Ito, *Sekiyu Gakkaishi* 36 (1993) 149.
- [12] H. Hamada, Y. Kintaichi, M. Inaba, M. Sasaki, T. Ito, M. Tabata, T. Yoshinari, K. Miyamoto, H. Tsuchida, in: *Abstracts of the 73rd CATSJ Meeting*, No. 2A2, Vol. 36, 1994, p. 2116.
- [13] H. Ohtsuka, T. Tabata, O. Okada, L.M.F. Sabatino, G. Bellussi, *Catal. Today* 42 (1998) 45.
- [14] H. Hamada, *Catal. Today* 22 (1991) 21.
- [15] J. Yan, M. Kung, W. Sachtler, H. Kung, *J. Catal.* 172 (1997) 178.
- [16] M. Sasaki, H. Hamada, Y. Kintaichi, T. Ito, *Catal. Lett.* 15 (1992) 297.
- [17] C. Li, K.A. Bethke, H.H. Kung, M.C. Kung, *J. Chem. Soc., Chem. Commun.* (1995) 813.
- [18] T. Maunula, Y. Kintaichi, M. Inaba, M. Haneda, K. Sato, H. Hamada, *Appl. Catal. B* 15 (1998) 291.
- [19] C. Li, C.W. Yan, Q. Xin, *Catal. Lett.* 24 (1994) 249.
- [20] H. Hamada, *Catal. Survey Jpn.* 1 (1997) 53.
- [21] R. Burch, T.C. Waitling, *Catal. Lett.* 37 (1996) 51.
- [22] M.F.L. Johnson, *J. Catal.* 123 (1990) 245.
- [23] Y. Ukisu, T. Miyadera, A. Abe, K. Yoshida, *Catal. Lett.* 39 (1996) 265.
- [24] Y. Ukisu, S. Sato, G. Muramatsu, K. Yoshida, *Catal. Lett.* 16 (1992) 11.
- [25] A.A. Davydov, *Kinet. Catal.* 35 (4) (1994) 608.
- [26] M.C. Kung, H.H. Kung, *Catal. Rev.-Sci. Eng.* 27 (3) (1985) 425.

- [27] N. Topsoe, H. Topsoe, *J. Catal.* 75 (1982) 354.
- [28] H.C. Yao, M. Shelef, in: R.L. Klemesch, J.G. Larson (Eds.), *The Catalytic Chemistry of Nitrogen Oxides*, Plenum Press, New York, 1975, p. 45.
- [29] A. Zecchina, E. Garrone, C. Morterraand, S. Coluccia, *J. Phys. Chem.* 79 (1975) 978.
- [30] E.L. Kugler, R.J. Kokes, J.W. Gryder, *J. Catal.* 36 (1975) 142.
- [31] J.M. van Doren, R.A. Morris, A.A. Viggiano, A.E.S. Miller, T.M. Miller, J.F. Paulson, *Int. J. Mass Spectrosc. Ion Processes* 117 (1992) 395.
- [32] G.R. Bamwenda, A. Obuchi, A. Ogata, J. Oi, S. Kushiyama, K. Mizuno, *J. Mol. Catal. A: Chem.* 126 (1997) 151.
- [33] V.A. Matyshak, O.V. Krylov, *Catal. Today* 25 (1995) 1.
- [34] N.W. Cant, A.D. Cowan, I.O.Y. Liu, A. Satsuma, in: *2nd World Congress on Environmental Catalysis*, 15–20 November 1998, Miami Beach.
- [35] H.-Y. Chen, T. Voskoboinikov, W.M.H. Sachtler, in: *2nd World Congress on Environmental Catalysis*, 15–20 November 1998, Miami Beach.
- [36] T. Beutel, B. Adelman, W.M.H. Sachtler, *Catal. Lett.* 37 (1996) 125.
- [37] N.W. Hayes, R.W. Joyner, E.S. Shpiro, *Appl. Catal. B* 8 (1996) 343.
- [38] T. Maunula, Y. Kintaichi, H. Hamada, *Catal. Lett.* 61 (1999) 121.